Designing isolated vanadium sites over mesoporous MCM-41:

Characterization and Catalytic applications

S. Shylesh, Surendran Parambadath and A.P.Singh*

Catalysis Division, National Chemical Laboratory, Pune- 411 008, India.

Corresponding author; Telefax No.: +91-20-25893761; E-mail:apsingh@cata.ncl.res.in :
ap.singh@ncl.res.in

Abstract: Vanadium-containing mesoporous molecular sieves were synthesized by three different routes viz. by the direct hydrothermal, grafting and immobilisation methods. The introduction of vanadium species as well as the nature of vanadium species formed over the MCM-41 support surface was probed by XRD, N_2 sorption isotherms, UV-VIS and TPR techniques. XRD, N_2 adsorption and TEM results show that the characteristic structural features of MCM-41 are preserved after surface modifications. Spectroscopic measurements reveal that vanadium exists mainly in tetrahedral positions for the hydrothermally synthesized catalyst while the grafting method tends the vanadium species to exist as higher coordinated species. Reaction data showed that the activity of the catalyst in the oxidation reaction of naphthalene is higher at high reaction temperatures and polar aprotic solvents like acetonitrile promotes the reaction drastically. The observed higher catalytic behaviour of the immobilized vanadium catalysts may result from the better active metal site isolation than the directly synthesized as well as grafted catalyst.

Key Words: Vanadium, Mesoporous, MCM-41, Oxidation, H_2O_2

1. Introduction

Molecular sieves containing transition metals had attracted great interest in catalytic oxidation process, especially in fine chemical synthesis (1-4). Vanadium- containing zeolitic molecular sieves and mesoporous materials were found to be active in a number of liquid phase oxidation reactions using H_2O_2 and TBHP as oxidants (5-8). A comparison of metal incorporated zeolitic molecular sieves with mesoporous materials shows that the activity and heterogenity of the zeolitic catalysts are far ahead of the mesoporous molecular sieves. However, the limited pore size of zeolites (2-20 Å) retards the transformation of bulkier organic molecules in their pore channels and hence M41S materials with large pore sizes (20-200 Å) receive wide utility in various catalytic applications.

Even though literature shows a broad spectrum of hydrothermally synthesized vanadium containing mesoporous catalysts (V-MCM-41), serious drawbacks of this procedure is the amount of metal incorporated is low (5-10). Contrary to the direct hydrothermal synthesis, grafting methods help to achieve a high percentage of metal

loading and also helps to disperse the active metal sites by suitably tuning the preparation procedures. Moreover, immobilized metal catalysts are reported to be more active and selective than direct synthesized catalysts, since the active metal sites are well isolated by the immobilization procedures and thus the leaching problem can also be minimized (4). However the nature of support interaction and the active metal site isolations is entirely different in all the three preparation procedures and hence a careful investigation is needed in order to design a better vanadium-containing mesoporous material.

In this paper the nature of vanadium species formed in mesoporous MCM-41 support surface by different synthesis protocols is described. For that purpose, a direct hydrothermally synthesized vanadium catalyst is compared with a grafted and an immobilized catalyst. The activity as well as the heterogenity of the catalysts is probed in the one-step liquid phase oxidation reaction of naphthalene using H_2O_2 as an oxidant.

2. Experimental

2.1. Synthesis Procedure

(a) Synthesis of vanadium-containing catalyst by direct hydrothermal method (V-MCM-41).

For the synthesis of V-MCM-41 catalyst, gel having a molar composition of

$$SiO_2 : 0.018VO_2 : 0.17Na_2O : 0.5CTMABr : 60H_2O$$
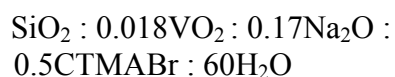
is used. Typically, required amounts of cetyl trimethyl ammonium bromide and vanadyl sulfate were added to a stirred solution mixture of fumed silica in alkaline condition. The mixture was then stirred at room temperature for 5 h and was then subsequently autoclaved at 100 °C for 4 days. For comparison, a silica polymorph was also prepared by the same method but with out the addition of vanadyl sulfate solution. The obtained material was washed with water and acetone, dried at 80 °C and finally calcined in air at 540 °C for 5 h.

(b) Synthesis of vanadium-containing catalyst by grafting method (V/MCM-41).

The grafting of vanadyl acetylacetonate on the mesoporous support was carried out by stirring 1 g of the support (dried at 100 °C/2 h) in an alcholic solution of VO (acac)$_2$ salt, so as to obtain a vanadium loading of 1 wt%. After addition, the solution was stirred at room temperature for 2 h and at 70 °C for 5 h and finally the sample was dried by removing the excess solvent using a rotary evaporator. Calcination procedure of the material was done as stated above for the synthesis of V-MCM-41.

(c) Synthesis of vanadium-containing catalyst by immobilization method (V-NH$_2$-MCM-41).

To a stirred suspension of 1 g of Si-MCM-41 in toluene (60 ml), 2.2 mmol of 3-amino propyl trimethoxy silane (3-APTS) was added slowly and was then allowed to stir overnight at 110 °C. The material was then filtered, washed with toluene, and then soxhlet extracted using a mixture of diethyl ether and dichloromethane for 24 h and dried under vacuum. The complexation of VO^{2+} ions on the organo modified silica surface was done by stirring a suspension of 1 g of the organo functionalised silica with a 0.01 M alcoholic solution of vanadyl sulfate for 5 h. The process was repeated twice for a maximum coordination of vanadyl groups on the functionalised silica

surface and then it was filtered, washed with copious amounts of ethanol and dried in an air oven at 80 ^{o}C for 3 h.

2.2. Characterization

Powder X-ray diffraction patterns of as-synthesized and calcined samples were recorded on a Rigaku D MAX III VC Ni-filtered Cu K$_{\alpha}$ radiation, λ=1.5404 Å, between 1.5 to 10° (2θ) with a scanning rate of 1°/min. The specific surface area, total pore volume and average pore diameter were measured by N$_2$ adsorption-desorption method using NOVA 1200 (Quanta chrome) instrument. The samples were activated at 200 ^{o}C for 3 h under vacuum and then the adsorption-desorption was conducted by passing nitrogen over the sample which was kept under liquid nitrogen. Pore size distribution (PSD) was obtained by applying the BJH pore analysis applied to the adsorption branch of nitrogen adsorption-desorption isotherms. TEM images were taken on a JEOL JEM-1200 EX instrument with 100 kV acceleration voltages to probe the mesoporosity of the material.

Diffuse reflectance UV-Vis spectra were recorded in the range 200-800 nm with a Shimadzu UV-2101 PC spectrometer equipped with a diffuse reflectance attachment, using BaSO$_4$ as the reference. The absorption edge energy values were determined by plotting $(\alpha h\nu)^{1/2}$ vs the excitation energy (α=absorption coefficient determined from the Kubelka-Munk function) and extrapolating the linear part of the curve to $(\alpha h\nu)^{1/2}=0$. Temperature programmed reduction was carried out on a Micromeritics Autochem 2910 catalyst characterization system, equipped with a TCD detector. The reduction was carried out in 5% H$_2$/Ar gas mixture flowing through the reactor at a rate of 20 ml/min and approximately 100 mg of the calcined sample was used for all the experiments. The temperature was then increased to 800 ^{o}C at a heating rate of 10 ^{o}C/min.

2.3. Catalytic reaction

Reactant mixtures of naphthalene (E-Merck), oxidant and acetonitrile (E-Merck) solvent were added to 0.1 g of catalyst and heated at a constant temperature of 80 ^{o}C under magnetic stirring. The typical molar ratio of the reactants was kept as: naphthalene:H$_2$O$_2$:solvent = 1:3:10. After reactions, the reaction mixture was cooled to room conditions and the catalyst was separated from the reaction mixture by centrifugation. The oxidised products were analyzed on a gas chromatograph (HP 6890) equipped with a flame ionization detector (FID) and a capillary column (5 μm cross linked methyl silicone gum, 0.2mm×50m) and were further confirmed by GC-MS (Shimadzu 2000 A).

3. Results and discussion

3.1. Powder X-ray diffraction

XRD patterns of Si-MCM-41, V-MCM-41, V-NH$_2$-MCM-41 and V/MCM-41 materials are given in Fig. 1. The well-defined XRD patterns of Si-MCM-41 and V-MCM-41 samples can be indexed to the Bragg reflections *100, 110, 200* and *210*, characteristic of materials with long range ordering and their intensities are well pronounced (5, 7). After calcination, a decreased intensity of the characteristic peak with a corresponding disappearance of long range ordered *210* peak is observed, showing a relatively well-ordered hexagonal structure of the materials. A slight shift of the characteristic (100) reflection to lower angle with a corresponding increase in the *d* spacing and a$_o$ values is noted after vanadium introduction than the corresponding silica polymorph (Table

1). The increase in the hexagonal unit cell parameter compared with the silica polymorph can be taken as an indication for the incorporation of vanadium, as the V-O bond distances are longer than the Si-O bond distances (7). Importantly, for V/MCM-41 and V-NH$_2$-MCM-41 samples a decrease in intensity of the characteristic *100* peak and a gradual loss in long range ordering are noted. These structural changes may arise from the inherent poor hydrothermal stability of M41S materials and thus high temperature treatments may dissociate some of the pore walls and thereby affects the long range ordering. We believe that the well ordered mesoporous structure obtained for the vanadium-incorporated V-MCM-41 catalyst may arise from the simultaneous condensation between metal and silicon species in presence of the organic micelles and thereby influencing the wall thickness and long range ordering of the final mesoporous material (7). However, for the grafted/immobilised catalyst systems since the metal species are mainly located on the surface, the aforementioned interactions are limited and hence influence the peak broadening with the loss of long range ordering. No bands characteristic of crystalline V$_2$O$_5$ phase is observed in any of the preparation methods and hence assumed that the metal ions were either atomically dispersed in the framework positions of MCM-41 or may exist in an amorphous dispersed form on the outside surface of mesoporous support.

3.2. N$_2$ adsorption-desorption measurements

The surface area of the catalysts determined by BET method shows that the surface area of all catalysts is in the range 700-900 m^2/g (Table 1). In detail, for the as synthesized V/MCM-41and V-NH$_2$-MCM-41 catalysts the surface area value decreased sharply from the support surfaces due to the presence of the bulkier organic moieties inside the pore channels. However, after calcination, the surface area of the impregnated and immobilised materials increased and retains 90% of the original value due to the removal of the bulky acetyl acetonate/propyl amino groups. N$_2$ adsorption-desorption isotherms of V-MCM-41 (55), V/MCM-41 and V-NH$_2$-MCM-41 materials show an inflection in the P/Po range of 0.2-0.4, with completely reversible isotherms but with little hysterisis characteristic for ordered mesoporous materials of Type IV according to the IUPAC classification (Fig. 2). Further, the BJH pore size distribution analysis of all samples shows sharp peaks in the range 20-30 Å attributed to well-defined mesopore structures (Table 1).
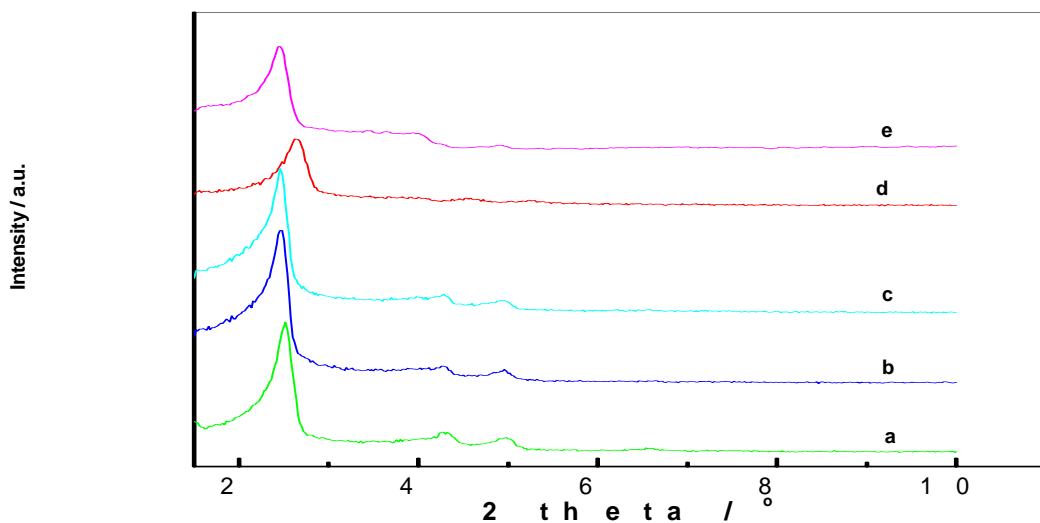
FIG. 1. X-ray diffraction patterns of (a) Si-MCM-41, (b) V/MCM-41 (as syn.), (c) V/MCM-41 (cal.), (d) V-MCM-41 and (e) V-NH$_2$-MCM-41.

TABLE 1

Characteristics of Vanadium-containing MCM-41 catalysts *

Catalyst	V (mmolg^{-1}) [a]	a_o [b] (Å)	S_{BET} m^{2}g^{-1}	Wall Thickness[c] (Å)	TPR [d] $T_{max.}$ (^{o}C)	AOS
Si-MCM-41	0.0	40.49	845	8.22	-	-
V/MCM-41 (C)	0.196	41.48	797	8.90	504	3.3
V-NH$_2$-MCM-41 (A)	0.281	41.14	342	11.51	n.e.	n.e.
V-NH$_2$-MCM-41 (C)	0.262	40.60	782	n.e.	501	3.4
V-MCM-41	0.192	39.31	909	15.72	412	4.5
Silica polymorph	0.0	36.51	711	14.52	-	-

[a]Vanadium content determined by ICP analysis.
[b] $a_o = 2d_{100}/\sqrt{3}$, [c]Wall thickness$=a_o-D_p$, where D_p is the pore diameter.
[d]Temperature of maximum hydrogen consumption ($T_{max.}$) and the average oxidation state (AOS) after reduction.
*Letter C and A in parenthesis means calcined and as-synthesized samples, n.e.=not evaluated.
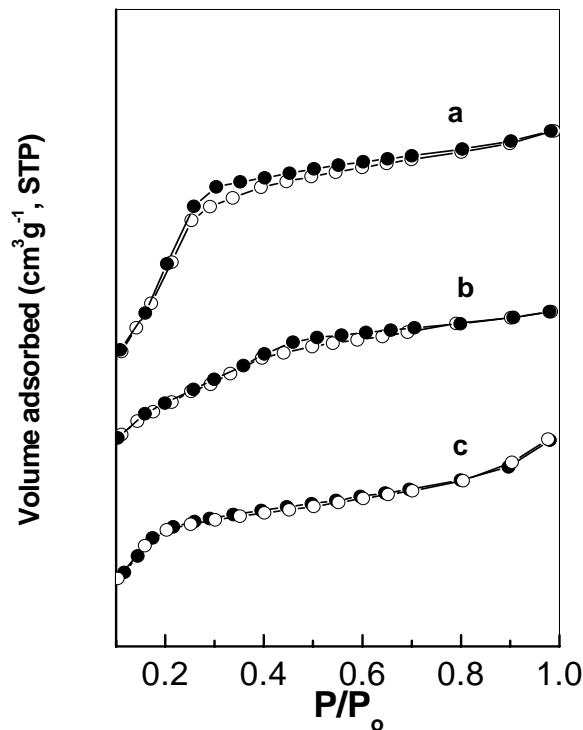
Fig. 2. Nitrogen adsorption-desorption isotherms of (a) V/MCM-41 (b) V-MCM-41 and (c) V-NH$_2$-MCM-41.

3.4. UV-VIS Spectroscopy
The UV-Vis spectra of Si-MCM-41, V-MCM-41, V/MCM-41 and V-NH$_2$-MCM-41 samples are given in Fig. 3. The band at 220 nm is typical for siliceous materials but new bands are appeared in the 250-500 nm range after vanadium incorporation. The as-synthesized V-MCM-41 catalysts are white in colour while V/MCM-41 and V-NH$_2$-MCM-41 are pale green in colour and on the basis of the appearance of green colour, weak absorptions in the longer wavelength can be interpreted (11). Even though the species anchored over the amino groups are V^{4+} in V-NH$_2$-MCM-41 catalysts, drying at 80 ^{o}C may change its oxidation state from +4 to +5, and hence the intensities of the UV-VIS peaks in the 600-800 nm regions are not so prominent and/or due to the low intense d-d transitions (10-30 times) than the high intense charge transfer (CT) transitions (6). Further, the colour of the dehydrated calcined catalysts (V-MCM-41, V/MCM-41) is white and on hydration (contact with atmosphere) the colour abruptly changes to yellowish for the V/MCM-41 catalysts. For V-MCM-41 catalyst its a slow process which may be due to the modification in the oxidation state of the vanadia species (V^{5+}) from the isolated tetrahedral coordination (T$_d$, 260 nm) to its square pyramidal coordination (O$_h$, 350-450 nm) by contacting with water molecules in the atmosphere. The possible and abrupt transition of calcined V/MCM-41

catalyst further indicates that a higher percentage of vanadium atoms are on the wall channels of V/MCM-41 and hence the water molecules can easily access the site for higher coordination. An attempt

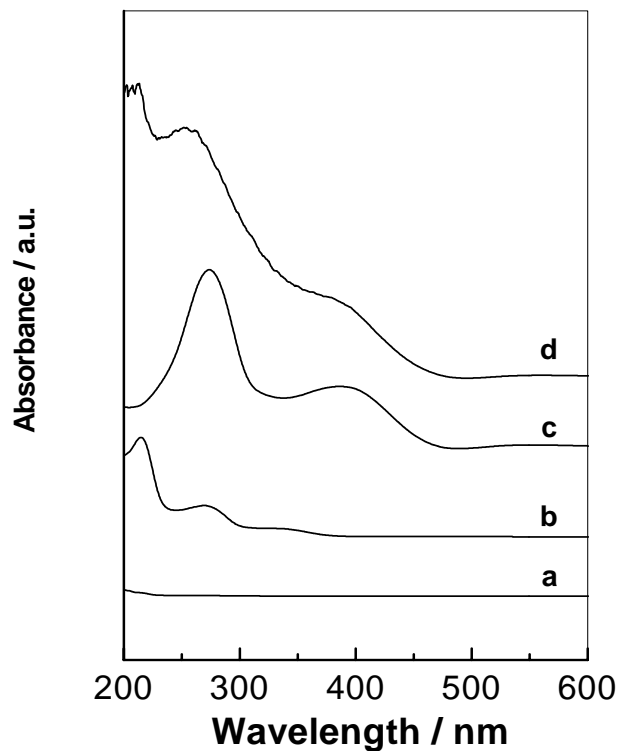was further made to investigate the local environment of vanadium in the MCM-41 surface by

Fig. 3. Diffuse reflectance UV-Vis spectra of (a) Si-MCM-41 (b) V-MCM-41 (c) V/MCM-41 and (d) V-NH$_2$-MCM-41.

performing the absorption edge energy measurements with reference to vanadium model compounds of known local symmetries (12). Usually the edge energy values of the V^{4+} are in the 4.5-5 eV energy region while the O^{2-} to V^{5+} ligand to metal charge transfer are in the 2-4 eV edge energy region (13). From table 2 and comparison with vanadium model compounds, it is apparent that all the edge energy values are in the range

2.5-3.5 eV. However, V-MCM-41 catalyst shows higher edge energy value than the grafted and immobilised calcined catalyst systems, showing the possible a decrease in vanadium domain size or a change in coordination of the vanadium cations. Thus vanadium ions in V-MCM-41 samples can be tentatively attributed to be tetrahedrally coordinated, supporting the framework incorporation.

TABLE 2

Absorption edge energy values of vanadium-containing mesoporous materials and vanadium-containing model compounds

Catalyst	Absorption edge energy value (eV)	Local symmetry
V/MCM-41	2.57	-
V-NH$_2$-MCM-41	2.60	-
V-MCM-41 (55)-H[a]	3.26	-
V-MCM-41 (55)-D[a]	3.40	-
V$_2$O$_5$	2.30	Square pyramidal
NH$_4$VO$_3$	3.23	Distorted tetrahedral
Na$_3$VO$_4$	3.21	Tetrahedral

a = H ; hydrated, D ; de-hydrated,

3.4. Temperature Programmed Reduction

H$_2$-TPR profiles of all the catalysts show that the reduction temperature maximum (T$_{max}$) and the average oxidation state (AOS) values vary considerably and are given in Table 1 and are shown in Fig. 4. The reduction profile of pure V$_2$O$_5$ is also included in figure 4 for comparison purpose. V-MCM-41 catalyst exhibits sharp reduction peaks at 685 K showing the reduction of monomeric or low oligomeric surface dispersed tetrahedral vanadia species (7). In sharp contrast to V-MCM-41 catalyst, V/MCM-41 material shows a very sharp peak at 783 K, and a distinct tail at ~843 K, indicating the formation of less reducible polymeric 'bulk-like' vanadia species (14). The TPR profiles of the immobilized calcined catalyst also show peak maximum at 778 K, but interestingly the profiles are devoid of the shoulder like peaks (~843 K), as observed with the grafted catalysts. Thus it can be pointed that the amino propyl groups in the immobilized catalyst inhibits the agglomerisation of the vanadia species and hence the formation of bulk-like vanadia species is not prominent. Thus the vanadium species incorporated in V-MCM-41 catalyst get reduced more easily than the vanadium grafted/immobilised catalyst systems.
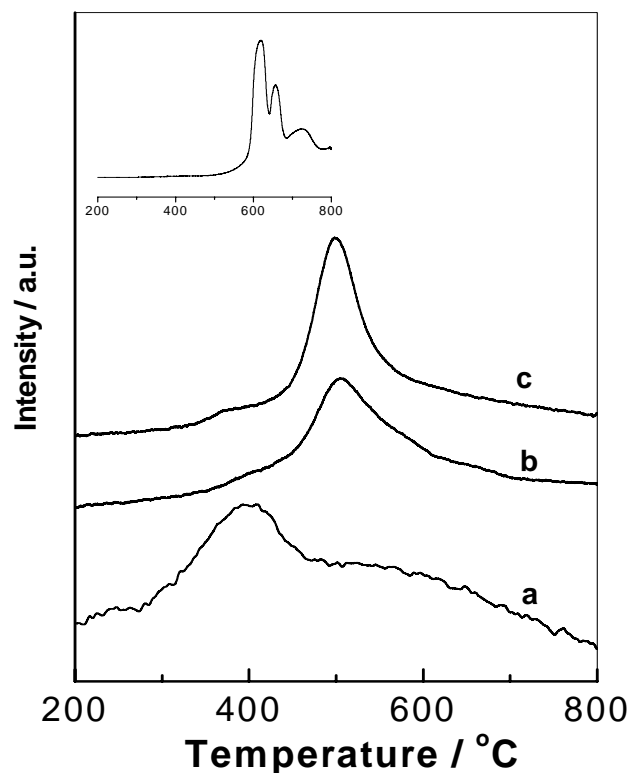
Fig. 4. H_2-TPR reduction profiles of (a) V-MCM-41 (b) V/MCM-41 (c) V-NH$_2$-MCM41 and insert pure V_2O_5.

3.5. Catalytic oxidation of naphthalene

Screening of the catalysts in the temperature range of 333-353 K shows that a higher temperature of 353 K helps to attain a maximum conversion rate with respect to substrate and the choice of oxidants follows that TBHP (70%) gives negligible reaction rate. However, shifting the oxidant from TBHP to dilute H_2O_2 (30%) increases the conversion rates drastically. In detail, the reaction rates obtained for V-MCM-41 and V-NH$_2$-MCM-41 catalysts systems show that the conversion increases gradually with time and reaches a maximum of 13.5% and 16.0%, respectively, after 24 h of the run. However, for the V/MCM-41 catalyst the conversions are abrupt at the early stages of the reaction and are almost steady through the run and show 16.4% naphthalene conversion after 24 h (Fig. 5).
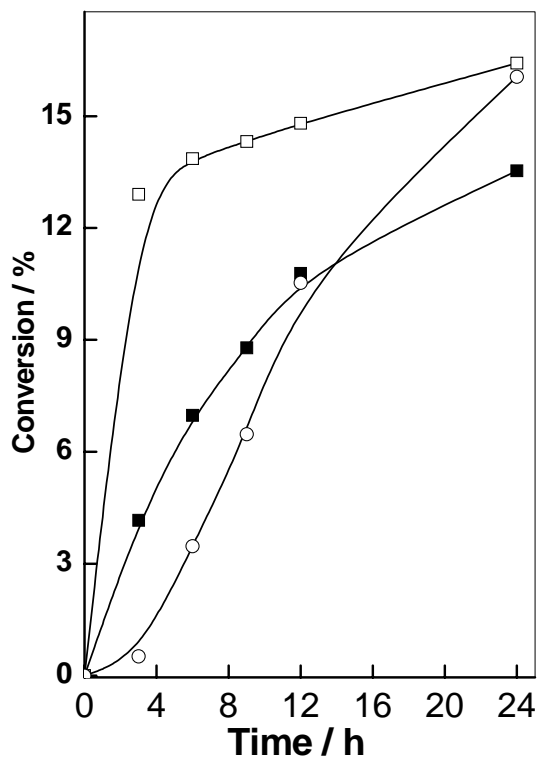
Fig. 5. Influence of reaction time in the conversion of naphthalene over (■) V-MCM-41, (□) V/MCM-41 and (O) V-NH$_2$-MCM-41.

Literature reveals that vanadium-containing mesoporous catalysts show leaching of active metal components during liquid phase oxidation reactions (6-9). Hence the heterogeneity of all the catalysts was investigated in detail using a series of leaching studies. According to Sheldon et al., the heterogenity of a catalyst can be better addressed if one compares the hot filtrate reaction mixtures for further conversion rates (15). Accordingly, resubmission of the filtrate under the reaction conditions (for V-MCM-41 and V/MCM-41) shows an enhancement in conversion rate, which shows that some of the vanadium atoms gets leached out during the run and thus the observed enhanced activity of the fresh catalysts may result from the leached vanadia species (Fig. 6A&B). The decreased heterogenity of the V-MCM-41 and V/MCM-41 catalysts can be related to the increased interaction of aqueous H$_2$O$_2$ (30 wt%) on the defect sites of the mesoporous material and thereby detach some of the vanadium species residing on the extra framework positions. Furthermore, the decreased heterogenity of the V-MCM-41 catalysts may arise from, (i) calcination treatments itself, as during calcination the water formed due to the decomposition of the template molecules can break some of the Si-O-V bonds, (ii) under drastic oxidation reaction conditions even the mesopore wall

54

structure itself gets collapsed and this may also contributes to the leaching of the vanadium species in a definite environment. These leached out vanadium species can interact with the water molecules present in the oxidant and can form well-homogenized different vanadium peroxo species and thus enhances the oxidation of the organic substrates faster as reaction progresses (7).
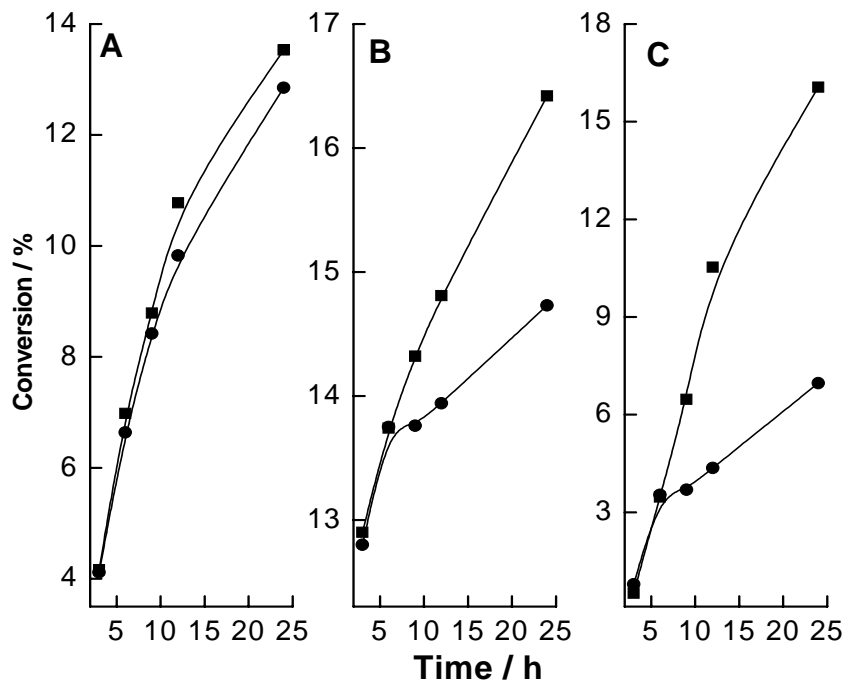

Fig. 6. Hot filtration experiments of different vanadium-containing MCM-41 samples (A) V-MCM-41, (B) V/MCM-41 and (C) V-NH$_2$-MCM-41; where (■) stands for fresh and (●) for filtration after 3h of the run.

On the contrary for the V-NH$_2$-MCM-41 catalyst, the high density amino groups on the mesoporous support surface tends to bind the VO^{2+} ions effectively and makes the immobilised catalyst more heterogeneous than the V-MCM-41 and V/MCM-41 catalysts (Fig. 6C). Thus the high catalytic performances as well as the increased stability of the immobilised catalysts arise from active metal site isolations and hence favour an easy approach for the reactants to the active extra framework metal sites. Moreover, the improved coordination ability of the amino groups in V-NH$_2$-MCM-41 catalyst system prevents the removal of the vanadia species, even during drastic reaction conditions and thereby points the novelty of anchored complex species for various oxidation reactions.

4. Conclusion

The surface property and activity difference of vanadium-substituted mesoporous material were compared with vanadium-grafted and vanadium-immobilised mesoporous MCM-41. Spectroscopic characterizations reveal that vanadium is incorporated inside the frame work positions of MCM-41 sample while the greater percentage of active species residing on the surface of post synthesis modified catalysts enhances the formation of higher coordinated vanadium species. Temperature programmed reduction measurement shows that vanadium species in V-MCM-41 are easily reducible than the V/MCM-41 catalyst and further shows the formation of polymeric-like vanadium species on the grafted calcined catalyst. Heterogenity studies prove that the activity of V-MCM-41 and V/MCM-41 catalysts arise from the presence of leached vanadium species while the activity of immobilized V-NH$_2$-MCM-41 is attributed to be arisen from a true heterogeneous catalyst.

Acknowledgement

References

[1]   Q. Zhang, Y. Wang, Y. Ohishi, T. Shishido, K. Takehira, J. Catal., 202 (2001) 308

[2]   H. Fujiyama, I. Kohara, K. Iwai, S. Nishiyama, S. Tsuruya, M. Masai, J. Catal., 188 (1999) 417.

[3]   J. Evans, A.B. Zaki, M.Y. El-Sheikh, S.A. El-Safty, J. Phys. Chem. B. 104 (2000) 10271.

[4]   W.A. Carvalho, M. Wallau, U. Schuchardt, J. Mol. Catal. A. Chem. 144 (1999) 91

[5]   J.S. Beck, J.C. Vartuli, W.J. Roth, M.E. Leonowicz, C.T. Kresge, K.D. Schmitt, C.T-W Chu, D.H. Olson, E.W. Sheppard, S.B. McCullen, J.B. Higgins, J.L. Schlenker, J. Am. Chem. Soc. 114 (1992) 10834.

[6]   J.S. Reddy, P. Liu, A. Sayari, Appl. Catal. A. Gen: 148 (1996) 7.

[7]   S. Shylesh, A.P. Singh, J. Catal. 228 (2004) 333.

[8]   D. Wei, W-T. Chuch, G. L. Haller, Catal. Today, 51 (1999) 501.

[9]   Z. Luan, J. Xu, H. He, J. Klinowski, L. Kevan, J. Phys. Chem., 100 (1996) 19595.

[10] Y. Deng, C. Lettmann, W.F. Maier, Appl. Catal. A. Gen: 214 (2001) 31.

[11] C-H. Lee, T-S. Lin, C-Y. Mou, J. Phys. Chem. B. 107 (2003) 2543.

[12] D.G. Barton, M. Shtein, R.D. Wilson, S.L. Soled, E. Iglesia, J. Phys. Chem. B. 103 (1999) 630.

[13] B. Olthof, A. Khodakov, A.T. Bell, E. Iglesia, J. Phys. Chem. B. 104 (2000) 1516.

[14] H. Berndt, A. Martin, A. Bruckner, E. Schreier, D. Muller, H. Kosslick, G.U. Wolf, B. Lucke, J. Catal. 191 (2000) 384.

[15] R. A. Sheldon, M. Wallau, I.W.C.E. Arends, U. Schuchardt, Acc. Chem. Res. 31 (1998) 485